

A model for the multiwavelength radiation from tidal disruption event Swift J1644+57

P. Kumar^{1*}, R. Barniol Duran^{2*}, Ž. Bošnjak^{3*} and T. Piran^{2*}

¹*Department of Astronomy, University of Texas at Austin, Austin, TX 78712, USA*

²*Racah Institute for Physics, The Hebrew University, Jerusalem, 91904, Israel*

³*Department of Physics, University of Rijeka, 51000 Rijeka, Croatia*

Accepted ; Received ; in original form February 15, 2013

ABSTRACT

Gamma-ray observations of a stellar tidal disruption event (TDE) detected by the Swift satellite and follow up observations in radio, mm, infrared and x-ray bands have provided a rich data set to study accretion onto massive black holes, production of relativistic jets and their interaction with the surrounding medium. The radio and x-ray data for TDE Swift J1644+57 provide a conflicting picture regarding the energy in relativistic jet produced in this event: x-ray data suggest jet energy declining with time as $t^{-5/3}$ whereas the nearly flat light curves in radio and mm bands lasting for about 100 days have been interpreted as evidence for the total energy output increasing with time. We show in this work that flat light curves do not require addition of energy to decelerating external shock (which produced radio and mm emission via synchrotron process), instead the flat behavior is due to inverse-Compton cooling of electrons by x-ray photons streaming through the external shock; the higher x-ray flux at earlier times cools electrons more efficiently thereby reducing the emergent synchrotron flux, and this effect weakens as the x-ray flux declines with time.

Key words: radiation mechanisms: non-thermal - methods: analytical - X-rays: bursts

1 INTRODUCTION

When a star wanders too close to a massive black hole it is shredded by the strong tidal gravity of the BH. In this process a fraction of the star is captured by the BH and is eventually accreted, and roughly half of the stellar mass is flung out on hyperbolic orbits (Lacy et al. 1982; Rees 1988; Evans & Kochanek 1989; Goodman & Lee 1989; Ayal, Livio & Piran 2000). Such an encounter is expected to occur at a rate of 10^{-3} – 10^{-5} yr⁻¹ per L_* galaxy (Magorrian & Tremaine 1999; Wang & Merritt, 2004; Bower, 2011). The accretion disk is expected to produce blackbody radiation in UV and soft x-ray bands from the region close to the BH, and a bright optical flash is produced by a super-Eddington outflow and by the irradiation and photo-ionization of unbound stellar debris (Strubbe & Quataert 2009, 2011).

Generation of a relativistic jet is also expected to accompany a tidal disruption event (TDE) as the stellar material bound to the BH gravity is accreted over a period of time; we know empirically that accreting BHs in active galactic nuclei (AGNs) produce jets moving at speed close to that of light with Lorentz factor of order 10. A number of theoretical ideas regarding jet generation and energy production in the context of TDEs have been explored in several

recent papers e.g., De Colle et al. 2012, Liu, Pe'er & Loeb 2012, Tchekhovskoy et al. 2013). The jet launched in a TDE interacts with the circum-nuclear medium (CNM) and produces synchrotron radiation over a broad frequency band from radio to infrared which Giannios & Metzger (2011) predicted should be observable for several years (also Metzger et al. 2012).

The NASA Swift satellite discovered a transient event, Swift J1644+57, in γ & x-ray bands two years ago (Burrows et al. 2011, Bloom et al. 2011) which was subsequently observed in radio, mm, infrared and x-ray bands for a time period of more than year with good temporal coverage, e.g. Zauderer et al. (2011), Levan et al. (2011), Berger et al. (2012), Saxton et al. (2012), Zauderer et al. (2013), and the data is broadly in line with expectations of a TDE, e.g. Burrows et al. (2011).

Two other transient events observed in the last year have also been suggested to be TDE (Cenko et al. 2011, Gezari et al. 2012). However, the follow up observations for these events have been sparse, and so we consider in this paper only Swift J1644+57 and the puzzle posed by the rich data set for this event.

The mm & radio light curves for Sw J1644+57 were found to be flat/rising for $\sim 10^2$ days by Berger et al. (2012). These authors suggested that this implies continuous injection of energy to the decelerating blast wave, which produced this radiation, for $\sim 10^2$ d. However, that requires about 20 times more energy in the

* E-mail: pk@astro.as.utexas.edu, rbarniol@phys.huji.ac.il, zeljka.bosnjak@cea.fr, tsvi.piran@mail.huji.ac.il

blast wave¹ than the initial jet energy that produced the strong X-ray signal which was of order 10^{52} erg. This energy requirement of more than a few times 10^{53} erg is very difficult to satisfy for a TDE model. We show in this paper that the multi-wavelength light curves of Sw J1644+57 can be understood without requiring energy in the blast wave to increase with time.

In the next section we describe the main features of the data for Swift J1644+57, and the main puzzles. We then describe in §3 the main idea of this paper that offers a simple solution to the puzzling data, and the application to Sw J1644+57 is provided in §4. Some concluding remarks about this event can be found in §5.

2 SWIFT J1644+57: SUMMARY OF OBSERVATIONS AND PUZZLES THEY HAVE POSED

Swift/XRT found that the x-ray flux from Sw J1644+57 varied rapidly on time scale $\delta t_{obs} \sim 10^2$ s, indicating that the emission was probably produced at a distance of order $2c\delta t_{obs}\Gamma_j^2 \lesssim 10^{15}$ cm; $\Gamma_j \lesssim 10$ is jet Lorentz factor. The average x-ray flux was roughly constant for the first 5 days, then dropped suddenly by a factor 50 during the next 3 days, and subsequently for $20d \lesssim t_{obs} \lesssim 500d$ it declined as $\sim t_{obs}^{-5/3}$ (Burrows et al. 2011; Berger et al. 2012; Zauderer et al. 2013). The x-ray flux then declined further by a factor ~ 170 between 500 days and 600 days (Zauderer et al. 2013). The spectrum in the 0.3–10 keV Swift/XRT band is reported to be a power law function — $f_\nu \propto \nu^{-\beta}$ — with index $\beta \sim 0.7$ during the first ~ 50 days and then decreasing to ~ 0.4 a few hundred days after the tidal disruption.

This transient event received extensive coverage at multiple mm and radio frequencies. Depending on the frequency band the light curve was found to rise, or remained nearly flat, during the first 100 days, and then declined as roughly t_{obs}^{-1} . The spectrum at low frequencies ($\lesssim 10^{10}$ Hz) rose as $\sim \nu^{1.5}$ which is roughly consistent with that expected of a synchrotron spectrum below the self-absorption frequency (ν_a). And the spectrum above the peak of f_ν fell off as $\sim \nu^{-0.7}$. The synchrotron self-absorption frequency (ν_a) underwent a dramatic decline by a factor of 10 between 5 and 10 days, and subsequently ν_a displayed a very slow decline over the next several hundred days. The flux at the peak of the spectrum fell off during 5–10 days by a factor ~ 3 , then increased by a factor ~ 4 during 10– 10^2 days (Berger et al. 2012). It should be noted that these peculiar behavior of the radio data during the period 5–10 days coincided with a sharp decline of the x-ray flux by a factor $\sim 10^2$, e.g. Burrows et al. (2011), Berger et al. (2012).

The event was also observed in the infrared K-band ($\sim 1.4 \times 10^{14}$ Hz) multiple times between 5 and 50 days, and the flux was found to decline during the first 5 days as $\sim t_{obs}^{-3}$ (Levan et al. 2011).

One of the main puzzles posed by the rich data for this event is that light curves in $\gtrsim 10$ GHz frequency bands, which lie above the synchrotron absorption and other characteristic frequencies, show a flat or a rising behavior when in fact according to the external forward shock model these light curves should be declining as $\sim t_{obs}^{-1}$, e.g. Meszaros & Rees (1994), Chevalier and Li (2000), Panaitescu

& Kumar (2000), Granot and Sari (2002). Energy injection to the decelerating external blast wave between 10 and 10^2 days by a factor ~ 20 has been invoked, e.g. Berger et al. (2012), to prevent the decline of the radio light curve during this time interval. This huge amount of energy added to the blast wave, however, leaves no x-ray foot print, and that clearly is very puzzling². The model we suggest — IC cooling of electrons by x-ray photons — avoids this problem because it requires no energy addition to the decelerating external shock to flatten radio/mm light curves.

Two other puzzles suggested by the data are the precipitous decrease of ν_a by a factor 10 between 5 and 10 days, and the rapid fall off of the infrared light curve during the same period.

3 INFLUENCE OF X-RAYS ON EXTERNAL SHOCK RADIATION

Basic idea: relativistic jet from the TDE interacts with the CNM (circum-nuclear medium) and drives a strong shock wave into it³. CNM electrons accelerated by the shock radiate synchrotron photons at radio and higher frequencies. These electrons are cooled by the IC scattering of x-ray photons streaming through the shocked plasma⁴ (these x-ray photons are the same radiation that was observed by the Swift satellite); see Fig. 1 for a schematic sketch of this scenario. Since the x-ray flux declines rapidly with time ($f_x \propto t^{-5/3}$ for $t \gtrsim 10$ days), the IC cooling of electrons also diminishes with time and this is what is responsible for transforming an otherwise declining light curve ($f_\nu \propto t_{obs}^{-1}$) to a flat or a rising light curve in radio/mm band; the IC cooling by x-rays turns out to be very effective in suppressing synchrotron radiation in mm/cm bands at early times, and this suppression gets weaker with time as the x-ray flux declines.

One other thing we should address here for those who might be thinking that the observed spectrum above the peak ($f_\nu \propto \nu^{-0.8}$) is too shallow to be consistent with a fast electron cooling model. The observed parameters of Swift J1644+57 are such that IC scatterings for electrons radiating above the peak takes place in the Klein-Nishina regime, and hence the shallow observed spectrum; detailed calculations are presented in §3.1 & 3.2.

Since the main component of our proposed idea to explain radio/mm light curve behavior is IC cooling of electrons in the external shock by the observed x-ray radiation, we begin the technical part of this section with a description of this process. We show that it is unavoidable that IC cooling by x-ray photons significantly modifies electron distribution in the external shock for Sw J1644+57. We also discuss whether IC scatterings take place in the Thomson or Klein-Nishina (K-N for short, from now on) regime.

² The x-ray light curve fell off as $t_{obs}^{-5/3}$ for $t_{obs} \gtrsim 5d$, and therefore according to the x-ray data most of the energy release in relativistic jet took place during the first 5 days.

³ A reverse shock propagating into the jet can also be produced in the CNM-jet interaction provided that the jet is not Poynting flux dominated, i.e. the ratio of energy flux carried by magnetic fields and the kinetic energy of matter (σ) is not much larger than 1. The mechanism described in this paper can also be applied to reverse shock emission. However, the external reverse-shock has difficulties explaining the observed flat radio/mm light curves.

⁴ X-rays observed by the Swift satellite must have passed through the external shock region as long as they are produced at the same, or smaller, radius as the external shock. The very high variability of the x-ray data — on timescale of order minutes — suggests that the x-ray radiation is likely produced at a distance much smaller than the external shock radius.

¹ Using simple relativistic equipartition arguments Barniol Duran & Piran (2013) have shown that in the context of a standard synchrotron scenario, without IC cooling of electrons, the requirement that the blast wave energy should increase with time during the first ~ 200 days in order to explain the radio light curve behavior, does not depend on the choice of the geometry of the jet, nor does it depend on the precise spectral fitting of the radio data.

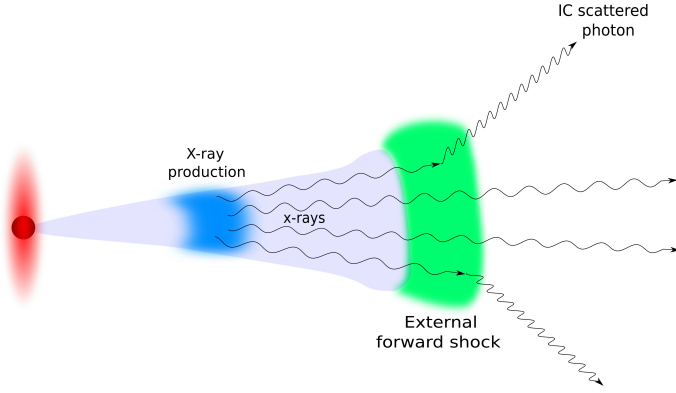


Figure 1. Shown here is a schematic sketch of a jet produced in TDE. The energy is converted into x-rays at some distance from the black-hole by an as yet unknown mechanism. A part of this x-ray radiation is scattered by electrons in the forward-external shock which results in their efficient cooling at early times.

Finally, we calculate electron distribution function when IC cooling due to an external x-ray radiation field occurs in the K-N regime.

3.1 Importance of IC cooling and its effect on electron distribution

Let us consider a x-ray radiation source with luminosity $L_x(t_{obs})$ (isotropic equivalent) in frequency band $\nu_1 - \nu_2$ which is produced by a source of size r_x . Its specific luminosity scales as $L_\nu \propto \nu^{-\beta}$; all unprimed variables are quantities measured in the rest frame of the host galaxy of the source. Now consider electrons in external forward shock at a radius $R(t_{obs})$, and the Lorentz factor of the shocked plasma (wrt CNM rest frame) to be $\Gamma(t_{obs})$. A photon of frequency ν moving at an angle θ wrt the radial direction is Doppler shifted to frequency ν' in shock comoving frame:

$$\nu' = \nu\Gamma(1 - \beta \cos \theta) \approx \frac{\nu}{2\Gamma} [1 + \theta^2 \Gamma^2], \quad (1)$$

where

$$\beta = (1 - \Gamma^{-2})^{1/2}, \quad (2)$$

and we used Taylor expansion for $\cos \theta$, and $\Gamma \gg 1$ to arrive at the approximate expression for ν' . From hereon all primed variables denote shock comoving frame.

The specific intensity in the host galaxy rest frame is

$$I_\nu(\theta) \approx \frac{L_\nu}{4\pi^2 r_x^2}, \quad (3)$$

for $\theta \lesssim r_x/R \equiv \theta_x$, and is zero otherwise. The specific intensity in the comoving frame of the shocked fluid is obtained by an appropriate Lorentz transformation, e.g. Rybicki & Lightman (1986), and is given by

$$I'_{\nu'} = I_\nu(\nu'/\nu)^3 \sim I_\nu/(8\Gamma^3), \quad (4)$$

when $\theta \ll \Gamma^{-1}$. Therefore, the specific flux in the comoving frame is

$$f'_{\nu'} \sim (\pi\theta_x'^2) I'_{\nu'} \sim \frac{L_\nu}{8\pi\Gamma R^2}, \quad (5)$$

where $\theta_x' \sim 2\Gamma\theta_x \ll 1$ is the angular size of the x-ray source as seen in the shock comoving frame. And the frequency integrated flux is

$$f'_x \sim \frac{L_x}{16\pi\Gamma^2 R^2}. \quad (6)$$

The factor Γ^2 in the denominator is easy to understand as it is due to Lorentz transformation of energy density.

The equation for IC cooling of an electron of Lorentz factor γ'_e is

$$\frac{d(m_e c^2 \gamma'_e)}{dt'_{ic}} = -\frac{4}{3} \sigma_T f'_x \gamma'^2_e, \quad (7)$$

where σ_T is Thomson scattering cross section. At the moment we are ignoring K-N effect which we will take up shortly. Thus, IC cooling time is given by

$$t'_{ic} \sim \frac{m_e c^2}{\sigma_T f'_x \gamma'_e} \sim (6 \times 10^6 \text{ s}) R_{17}^2 L_{x,47}^{-1} (\Gamma^2 / \gamma'_e), \quad (8)$$

where we made use of equation (6) for f'_x , and have adopted the widely used notation $X_n \equiv X/10^n$. The IC cooling calculation assumed that the external shock region is optically thin for x-ray photons. This condition is easily satisfied since the optical depth to Thomson scattering is $\sim \sigma_T n_e R \sim 10^{-7} n_e R_{17} \ll 1$ as long as n_e , the particle density in the unshocked CNM, is less than 10^7 cm^{-3} at a distance of 10^{17} cm from the black hole which is indeed the case as shown by radio observations. Also, absorption of x-ray photons by the inverse-Synchrotron process is negligibly small.

The dynamical time in the comoving frame is $t'_{dy} \sim R/(c\Gamma)$. Therefore,

$$\frac{t'_{ic}}{t'_{dy}} \sim \frac{2\Gamma^3 R_{17}}{\gamma'_e L_{x,47}}. \quad (9)$$

The Lorentz factor of the external shock a week after the tidal disruption is about 2 (see §3.2 for shock dynamics), $R_{17} \sim 1$, and $L_x \sim 5 \times 10^{46} \text{ erg/s}$. Thus we see from the above equation that the IC cooling time for electrons with $\gamma'_e \gtrsim 30$ is shorter than the dynamical time. Radio and mm photons observed from Sw J1644+57 are produced via synchrotron process by electrons with $\gamma'_e \gtrsim 50$, and so IC cooling cannot be ignored in the calculation of external shock radiation from this event. It should be pointed out that the synchrotron cooling is less important than the IC cooling at least for those electrons that are radiating well below the infrared band⁵.

For electrons with $\gamma'_e \lesssim 10^2$ the IC scatterings take place in the Thomson regime for Sw J1644+57. The reason is that the energy of a 10 keV photon — Swift/XRT energy band is 0.3–10 keV — in the electron comoving frame is $(10\gamma'_e/\Gamma)$ keV which is less than $m_e c^2$ as long as $\gamma'_e \lesssim 10^2$. Higher energy electrons scatter 10 keV photons with a reduced cross-section⁶, and the scattered photon energy is less than it is in the Thomson regime, i.e. $< \nu' \gamma'^2_e$. These two effects reduce the IC cooling of electrons with $\gamma'_e \gtrsim 10^2$. A simple, and fairly accurate, way to include these effects in IC cooling calculations is by only considering energy density in radiation field up to a photon energy of ϵ'_{kn} :

$$\epsilon'_{kn} \sim m_e c^2 / \gamma'_e \quad \text{or} \quad \nu'_{kn} = \epsilon'_{kn}/h, \quad (10)$$

⁵ The ratio of IC and synchrotron cooling times, in Thomson scattering regime, is equal to the ratio of energy density in magnetic field and radiation field. The x-ray luminosity from Sw J1644+57 was very high for the first several weeks, and thus it turns out that the energy density in radiation is much larger than magnetic energy density as long as ϵ_B for the shocked fluid is smaller than 1.

⁶ Klein-Nishina cross-section is smaller than the Thomson cross section by a factor of photon energy in electron rest frame divided by $m_e c^2$.

where h is Planck's constant. The spectral index in the x-ray band for Swift J1644+57 is $\beta \approx 0.7$, and in that case the reduction to the IC cooling due to K-N effect scales as $\gamma_e'^{-0.3}$ for large γ_e' (see §3.1.1). This is a weak effect but has important implications for electron distribution function which is discussed below.

3.1.1 Electron distribution function in external shock

Electron distribution function, $dn_e/d\gamma_e$, in a shocked plasma is determined by the dual effect of acceleration at the shock front and IC and synchrotron coolings while electrons travel down-stream. The distribution function is obtained from the following equation:

$$\frac{\partial}{\partial t} \frac{dn_e}{d\gamma_e} + \frac{\partial}{\partial \gamma_e} \left[\dot{\gamma}_e \frac{dn_e}{d\gamma_e} \right] = S(\gamma_e), \quad (11)$$

where

$$\dot{\gamma}_e = -\frac{4\sigma_T}{3m_e c^2} \left[f(< \nu_{kn}) + \frac{B^2 c}{8\pi} \right] \gamma_e^2 \beta_e^2, \quad (12)$$

is the rate of change of γ_e due to IC and synchrotron losses, $f(< \nu_{kn})/c$ is energy density in radiation below the K-N frequency ν_{kn} (eq. 10), and

$$S(\gamma_e) \propto \gamma_e^{-p} \quad \text{for } \gamma_e \geq \gamma_i \quad (13)$$

is the rate at which electrons with LF γ_e are injected into the system; γ_i is the minimum Lorentz factor for shock accelerated electrons. All the variables considered in this subsection are in shock comoving frame. However, we will not use prime (') on variables in this sub-section (and only in this sub-section) to denote shock comoving frame as this is the only frame being considered here. When results from this sub-section are used elsewhere in the paper we will revert back to the proper notation for prime and un-prime frames.

Let us define radiative cooling time

$$t_c(\gamma_e) = \frac{\gamma_e}{\dot{\gamma}_e}, \quad (14)$$

and cooling Lorentz factor, γ_c , which is such that

$$t_c(\gamma_c) \equiv t_{dy}, \quad (15)$$

where t_{dy} is the dynamical time.

We will calculate the distribution function in two cases. The slow cooling case where $\gamma_c > \gamma_i$, and the fast cooling regime when $\gamma_c < \gamma_i$. Moreover, we will consider here only IC losses in K-N regime as that is relevant for the “afterglow” radiation of the TDE Swift J1644+57. We note that the theoretical light curves and spectra shown for this event in the next section are obtained by numerical solutions of relevant equations that include synchrotron loss and no assumption regarding K-N regime.

Since $\nu_{kn} \propto \gamma_e^{-1}$ (eq. 10) and $f(< \nu_{kn}) \propto \gamma_e^{-(1-\beta)}$, therefore $\dot{\gamma}_e \propto \gamma_e^{1+\beta}$. We see from equation (11) that for $\gamma_e < \gamma_i$

$$\frac{dn_e}{d\gamma_e} \propto \frac{1}{\dot{\gamma}_e} \quad (16)$$

whereas for $\gamma_e > \gamma_i$

$$\frac{dn_e}{d\gamma_e} \propto \frac{\int_{\gamma_e}^{\infty} d\gamma S(\gamma)}{\dot{\gamma}_e}. \quad (17)$$

Therefore, the solution of equation (11) in the slow cooling case is

$$\frac{dn_e}{d\gamma_e} \propto \begin{cases} \gamma_e^{-p} & \gamma_i \leq \gamma_e \leq \gamma_c \\ \gamma_e^{-p-\beta} & \gamma_e > \gamma_c \end{cases} \quad (18)$$

and in the fast cooling case

$$\frac{dn_e}{d\gamma_e} \propto \begin{cases} \gamma_e^{-1-\beta} & \gamma_c \leq \gamma_e \leq \gamma_i \\ \gamma_e^{-p-\beta} & \gamma_e > \gamma_i \end{cases} \quad (19)$$

The synchrotron spectrum for particle distribution $dn_e/d\gamma_e \propto \gamma_e^{-q}$ is $f_\nu \propto \nu^{-(q-1)/2}$ for $\nu > \min(\nu_c, \nu_i)$, and it is $\nu^{1/3}$ for $\nu < \min(\nu_c, \nu_i)$; these spectra are modified when synchrotron-absorption becomes important (the criterion for this is discussed in the next sub-section)⁷.

It should be clear from these equations that the spectral index above the peak depends on p , and the spectral index β of the radiation field that is responsible for IC cooling of electrons; the spectral index for $\nu > \max(\nu_i, \nu_c)$ is $(p-1+\beta)/2$ which is harder than $\nu^{-p/2}$. As an application to Swift J1644+57 we note that the spectral index in the radio band above the peak of the spectrum is reported to be ~ 0.75 for $t_{obs} \gtrsim 10^2$ d (Berger et al. 2012). This does not mean that $p = 2.5$ as suggested by eg. Berger et al. If IC cooling in K-N regime is important for determining particle distribution, which equation (9) for t'_{ic}/t'_{dy} makes clear is the case, then $p = 2.3$, since according to the late time X-ray data $\beta = 0.4$ (Saxton et al. 2012).

3.2 Shock dynamics and synchrotron light curves

The dynamics of external forward shock can be determined, approximately, from the following energy conservation equation

$$\frac{4\pi}{(3-s)} R^3 R_{17}^{-s} n_f m_p c^2 \Gamma(\Gamma-1) = E, \quad (20)$$

where E is the energy (isotropic equivalent) in the blast wave, the density of the CNM is taken to be

$$n(R) = n_f R_{17}^{-s}, \quad (21)$$

and $R_{17} = R/10^{17}$ cm. For a relativistic shock, i.e. $\Gamma \gg 1$, the dynamics is described by

$$\Gamma = \left[\frac{(3-s)E_{51}}{4\pi m_p c^2 n_f R_{17}^{3-s}} \right]^{1/2}, \quad (22)$$

and the deceleration radius – where the relativistic ejecta has imparted roughly half its energy to the surrounding medium – is

$$R_{d,17} = \left[\frac{(3-s)E_{51}}{4\pi m_p c^2 n_f \Gamma_0^2} \right]^{1/(3-s)}, \quad (23)$$

where Γ_0 is the initial Lorentz factor of the relativistic outflow. For a non-relativistic shock the solution of equation (20) is

$$v = \left[\frac{(3-s)E_{51}}{2\pi m_p n_f R_{17}^{3-s}} \right]^{1/2}. \quad (24)$$

The Lorentz factor for the external shock of TDE Swift J1644+57 was of order a few at early times (less than a week), and the shock speed decreased to Newtonian regime at late times. Hence the analytical calculations we present in this section considers both of these regimes. The numerical results described in the next section are more accurate and do not rely on making any assumption regarding Γ .

A photon released at radius R arrives at the observer at time

⁷ A very detailed description of synchrotron spectrum when IC cooling in K-N regime is important can be found in Nakar et al. (2009)

$$t_{obs} = \frac{(1+z)}{c} \int dR \left[\frac{c}{v} - 1 \right]. \quad (25)$$

For relativistic blast waves $t_{obs} \propto R^{4-s}$, and for non-relativistic case $t_{obs} \propto R^{(5-s)/2}$. Moreover, the shock speed as viewed by an observer is

$$\Gamma \propto t_{obs}^{-\frac{3-s}{8-2s}} \quad \text{and} \quad R \propto t_{obs}^{1/(4-s)}, \quad (26)$$

for the relativistic case and

$$v \propto t_{obs}^{-\frac{3-s}{5-s}} \quad \text{and} \quad R \propto t_{obs}^{2/(5-s)}, \quad (27)$$

for Newtonian dynamics.

The deceleration time in observer frame, for relativistic outflow, is given by

$$t_d \approx (3 \times 10^4 \text{ s}) \left[\frac{(3-s)E_{53}}{1.8 n_{f,2}} \right]^{\frac{1}{3-s}} (1+z) \Gamma_{0,1}^{-\frac{8-2s}{3-s}}. \quad (28)$$

Thus, for $E = 10^{53} \text{ erg}$, $n_f = 10^2 \text{ cm}^{-3}$, and $\Gamma_0 = 10$, the deceleration time is of order 5 hours, and the Lorentz factor of the shocked CNM 10 days after the start of TDE is ~ 2 .

3.2.1 External shock radiation and light curves

We provide analytical calculation for synchrotron radiation and light curves from external forward shock in this sub-section; more accurate numerical results are presented in the next section.

The magnetic field strength and the electron minimum Lorentz factor in a shock heated plasma are estimated by assuming that a fraction of the energy of shocked plasma (ϵ_B) goes into the generation of magnetic fields, and a fraction (ϵ_e) is taken up by electrons⁸. Under this assumption we find that

$$B' = [32\pi\epsilon_B m_p c^2 n(R) \Gamma(\Gamma-1)]^{1/2}, \quad (29)$$

and the minimum Lorentz factor of shock accelerated electrons is

$$\gamma'_i = \frac{(p-2)m_p}{(p-1)m_e} \epsilon_e (\Gamma-1) \quad (30)$$

Using results for shock dynamics from last sub-section we find

$$B' \propto \begin{cases} t_{obs}^{-\frac{3}{2(4-s)}} & \Gamma\beta \gg 1 \\ t_{obs}^{-\frac{3}{5-s}} & \Gamma\beta \ll 1 \end{cases} \quad (31)$$

and the synchrotron frequency corresponding to electron Lorentz factor γ'_i is

$$\nu_i = \frac{qB'\gamma_i'^2 \Gamma}{2\pi m_e c(1+z)} \propto \begin{cases} t_{obs}^{-3/2} & \Gamma\beta \gg 1 \\ t_{obs}^{-\frac{15-4s}{5-s}} & \Gamma\beta \ll 1 \end{cases} \quad (32)$$

We next calculate synchrotron frequency for those electrons that cool on a dynamical timescale (ν_c) due to IC scattering of x-ray photons. Let us rewrite equation (7) to explicitly consider x-ray flux below the K-N frequency

$$\frac{dm_e c^2 \gamma'_e}{dt'_{ic}} = -\frac{4}{3} \sigma_T f'_x(< \nu'_{kn}) \gamma_e'^2, \quad (33)$$

⁸ This crude approximations is made due to our inability to calculate magnetic fields and electron acceleration in collisionless shocks ab initio. And the dimensionless parameters ϵ_B and ϵ_e hide our ignorance regarding these processes.

where ν'_{kn} is given by equation (10) for electrons of LF γ'_e . The LF of electrons that cool on a dynamical time is obtained from the above equation

$$\gamma'_e \sim \frac{3m_e c^2}{4\sigma_T f'_x(< \nu'_{kn}) t'_{dy}}. \quad (34)$$

For a power law spectrum for x-ray radiation

$$f'_x(< \nu'_{kn}) = \frac{L_x(< \nu_{kn})}{16\pi\Gamma^2 R^2} \propto \frac{L_x(t_{obs})}{R^2 \Gamma^{1+\beta} \gamma_e'^{1-\beta}}. \quad (35)$$

Therefore, the electron “cooling” Lorentz factor is given by

$$\gamma'_e \propto \left[\frac{R^2 \Gamma^{1+\beta}}{t'_{dy} L_x(t_{obs})} \right]^{1/\beta}, \quad (36)$$

Using equations for shock dynamics from last sub-section we find

$$\gamma'_e \propto \begin{cases} \left[\frac{t_{obs}^{[2-(2+\beta)(3-s)]/[2(4-s)]}}{L_x(t_{obs})} \right]^{1/\beta} & \text{for } \Gamma\beta \gg 1 \\ \left[\frac{t_{obs}^{(s-1)/(5-s)}}{L_x(t_{obs})} \right]^{1/\beta} & \text{for } \Gamma\beta \ll 1 \end{cases} \quad (37)$$

The synchrotron frequency in observer frame corresponding to γ'_e is

$$\nu_c = \frac{qB'\gamma_e'^2 \Gamma}{2\pi(1+z)m_e c^2}. \quad (38)$$

Or

$$\nu_c \propto \begin{cases} t_{obs}^{-3/2} \left[\frac{t_{obs}^{(s-2)/(4-s)}}{L_x(t_{obs})} \right]^{2/\beta} & \text{for } \Gamma\beta \gg 1 \\ t_{obs}^{-3/(5-s)} \left[\frac{t_{obs}^{(s-1)/(5-s)}}{L_x(t_{obs})} \right]^{2/\beta} & \text{for } \Gamma\beta \ll 1 \end{cases} \quad (39)$$

For $s = 1.5$, $\beta = 0.7$ and $L_x \propto t_{obs}^{-5/3}$ we find $\nu_c \propto t_{obs}^{2.7}$ for relativistic case, and $\nu_c \propto t_{obs}^{4.3}$ for Newtonian dynamics. For these parameters for Sw J1644+57, ν_c is about 1 GHz at 10 days, and it rises to 100 GHz at ~ 70 days.

The observed flux at a frequency $\nu > \max(\nu_a, \nu_i, \nu_c)$ is given by

$$f_\nu(t_{obs}) = f_p \nu_c^{\beta/2} \nu_i^{(p-1)/2} \nu^{-(p+\beta-1)/2}, \quad (40)$$

where ν_a is synchrotron absorption frequency,

$$f_p \approx \frac{q^3 B' \Gamma N_e}{m_e c^2} \frac{1+z}{4\pi d_L^2}, \quad (41)$$

$N_e \propto R^{3-s}$ is the total number of electrons with Lorentz factor $> \min(\gamma'_i, \gamma'_c)$, and d_L is the luminosity distance to the source; we made use of equations (18) and (19) in deriving equation (40).

Making use of equations (26), (27), (31), (32) and (39) in the above expression for f_ν we find the observed light curve behavior:

$$f_\nu(t_{obs}) \propto \frac{\nu^{-(p+\beta-1)/2}}{L_x(t_{obs})} \times \begin{cases} t_{obs}^{-[2+3\beta+3(p-1)]/4} & \Gamma\beta \gg 1 \\ t_{obs}^{-\frac{19-6s-p(15-4s)-3\beta}{2(5-s)}} & \Gamma\beta \ll 1 \end{cases} \quad (42)$$

For $p = 2.0$, $\beta = 0.7$, $s = 1.5$ and $L_x \propto t_{obs}^{-5/3}$, $f_\nu \propto \nu^{-0.85} t_{obs}^{-0.1}$ for relativistic dynamics, and $f_\nu \propto \nu^{-0.85} t_{obs}^{0.2}$ for Newtonian

shock. The dynamics of Swift J1644+57 for $10\text{d} \lesssim t_{\text{obs}} \lesssim 10^2\text{d}$ lies between these two extremes, and the light curve is flat for as long a duration as the observing stays above ν_c . Of course, at sufficiently high frequencies — which of order 10^{13}Hz for this TDE at $\sim 10\text{d}$ — electron cooling by IC scattering becomes unimportant due to K-N suppression, and synchrotron cooling time becomes smaller than the dynamical time. In this case the light curve decline has the well known form of $f_\nu \propto \nu^{-p/2} t_{\text{obs}}^{-(3p-2)/4}$ for relativistic shocks, e.g. Kumar (2000).

The rapid increase of ν_c with time is responsible for the nearly flat light curve observed for Swift J1644+57 in frequency bands $\nu > \max(\nu_a, \nu_i, \nu_c)$. When $\nu_c(t_{\text{obs}})$ moves above the observing band then the light curve resumes its usual, $\sim t_{\text{obs}}^{-1}$, decline which occurs at $t_{\text{obs}} \gtrsim 10^2\text{days}$ for $\nu \gtrsim 10^2\text{GHz}$ as shown in numerically calculated light curves presented in the next section.

Another interesting case to consider is when $\nu_c < \nu < \nu_i$ and the observing band is above the synchrotron absorption frequency. The light curve in this case is determined from

$$f_\nu(t_{\text{obs}}) = f_p \nu^{-\beta/2} \nu_c^{\beta/2}. \quad (43)$$

Making use of equations (41) and (39) we find

$$f_\nu(t_{\text{obs}}) \propto \frac{\nu^{-\beta/2}}{L_x(t_{\text{obs}})} \begin{cases} t_{\text{obs}}^{-(2+3\beta)/4} & \Gamma\beta \gg 1 \\ t_{\text{obs}}^{[4-2s-3\beta]/[2(5-s)]} & \Gamma\beta \ll 1 \end{cases} \quad (44)$$

For $\beta = 0.7$, $s = 1.5$ and $L_x \propto t_{\text{obs}}^{-5/3}$ the light curve rises as $\nu^{0.35} t_{\text{obs}}^{0.64} (t_{\text{obs}}^{1.5})$ for relativistic (Newtonian) blast waves.

Next, we calculate the synchrotron self-absorption frequency (ν_a) when IC cooling is important. The easiest way to determine ν_a is by using Kirchhoff's law or the fact that the emergent flux at frequency ν_a is approximately equal to the black-body flux corresponding to electron temperature given by

$$kT'_e = \max[\gamma'_a, \min(\gamma'_i, \gamma'_c)] m_e c^2 / 3, \quad (45)$$

where γ'_a is electron Lorentz factor corresponding to synchrotron frequency ν'_a , i.e. $\gamma'_a \propto (\nu'_a/B')^{1/2}$. The equation for ν'_a , using Kirchhoff's law, is

$$\frac{2kT'_e \nu_a'^2}{c^2} \approx \frac{\sigma_T B' m_e c^2 N_e(> kT_e/m_e c^2)}{4\pi q}, \quad (46)$$

where the left side of this equation is the Planck function in the Rayleigh-Jeans limit, and $N_e(> kT_e/m_e c^2)$ is the column density of electrons with LF larger than $\max[\gamma'_a, \min(\gamma'_i, \gamma'_c)]$.

One case of particular interest for application to Sw J1644+57 is where ν_a is larger than $\max(\nu_i, \nu_c)$. We can rewrite equation (46) for this case as

$$2m_e \nu_a'^{5/2} \left(\frac{2\pi m_e c}{qB'} \right)^{1/2} = f'(\nu'_a) = \frac{f_{\nu_a} d_L^2}{\Gamma R^2}. \quad (47)$$

Making use of equations (26), (27), (31) and (42) we find

$$\nu_a \propto \begin{cases} \frac{t_{\text{obs}}^{-\frac{8+(4-s)(3p+3\beta+2)}{2(4-s)(p+\beta+4)}}}{L_x^{\frac{2}{p+\beta+4}}} & \Gamma\beta \gg 1 \\ \frac{t_{\text{obs}}^{-\frac{30-6s-p(15-4s)-3\beta}{(5-s)(p+\beta+4)}}}{L_x^{\frac{2}{p+\beta+4}}} & \Gamma\beta \ll 1 \end{cases} \quad (48)$$

For $s = 1.5$, $p = 2$, $\beta = 0.7$, and $L_x \propto t_{\text{obs}}^{-5/3}$, $\nu_a \propto t_{\text{obs}}^{-0.49} (t_{\text{obs}}^{0.45})$ for relativistic (Newtonian) shock dynamics. We note that due to the rapid rise of ν_c (see eq. 39) the above equation for ν_a

ceases to be applicable after a few tens of days for Sw J1644+57 when the ordering of synchrotron characteristic frequency changes to $\nu_i < \nu_a < \nu_c$. The synchrotron absorption frequency for this case can be shown to be

$$\nu_a \propto \begin{cases} \frac{t_{\text{obs}}^{-\frac{1}{p+4} \left[\frac{10-s}{2(4-s)} + \frac{3(p-1)}{2} \right]}}{t_{\text{obs}}} & \Gamma\beta \gg 1 \\ \frac{t_{\text{obs}}^{-\frac{[(5+4s)+(15-4s)(p-1)]}{(5-s)(p+4)}}}{t_{\text{obs}}} & \Gamma\beta \ll 1 \end{cases} \quad (49)$$

For $s = 1.5$ and $p = 2$, $\nu_a \propto t_{\text{obs}}^{-0.53} (t_{\text{obs}}^{-0.95})$ for relativistic (Newtonian) shock dynamics.

The rise of light curve for about 10^2days for $\nu \lesssim 10\text{GHz}$ is due to the fact that these observing bands lie below the synchrotron absorption frequency during this period. The observed flux below ν_a decreases rapidly with decreasing ν , and hence even a slow decrease of ν_a with time leads to a rising light curve.

4 NUMERICAL RESULTS AND APPLICATION TO SWIFT J1644+57

Equations (20) & (25) are solved numerically to determine shock dynamics as a function of observer time, and equations (11), (12), (29), (30) & (46) are used for calculating spectra and light curves that take into account electron cooling due to IC scattering of an “external” radiation field with flux and spectrum taken from x-ray observations, and also cooling due to synchrotron radiation. No assumption regarding whether IC scatterings are in K-N or Thomson regime are made for calculations presented in this section.

The energy in the blast wave is injected only at the beginning of numerical calculation when the blast wave is at a radius $R = 10^{13}\text{cm}$; results are insensitive to the precise value of the initial radius as long as it is taken to be much smaller than the deceleration radius. In Fig. 2 we show R , Γ , B' , γ_i & γ_c , for parameters relevant for Sw J1644+57.

Theoretically computed light curves for Sw J1644+57 in frequency bands 230 GHz & 87 GHz, together with observed data from Berger et al. (2012), are shown in Fig. 3. The theoretical light curves were calculated from a decelerating blastwave which had a fixed amount of total energy (i.e. no late time injection of energy) and yet the observed flux in these frequency bands is nearly flat for $\sim 10^2\text{days}$ (consistent with the observed data) in spite of the fact that these bands clearly lie above the synchrotron injection (ν_i) and self-absorption (ν_a) frequencies (shown in fig. 4). There is a noticeable dip in light curves between ~ 10 & 20 days. The reason for this dip is that the observed x-ray light curve during this period is nearly flat (except, of course, for the ever present fluctuations). A flat x-ray light curve means that ν_c does not change much during this time interval (see fig. 4). However, ν_i and the peak flux (which are independent of L_x) continue their monotonic decline, and that is the reason for the flux decrease during this period. A more realistic treatment of the x-ray flux in our calculation, that includes the observed fluctuations, should provide a better fit to the observed data.

The nearly flat light curves for $\sim 10^2$ days for 87 and 230 GHz is due to the fact that these bands lie above the synchrotron cooling frequency which rises very rapidly with time ($\nu_c \propto t_{\text{obs}}^3$) due to the rapidly declining x-ray flux; we obtained this behavior analytically in the last section, and the numerical result is presented in fig. 4. The light curve remains nearly flat as long as the observing band is above ν_c , and then it starts to decline as $\sim t_{\text{obs}}^{-1.8}$. The duration of the flat phase is dictated by the temporal behavior of x-ray

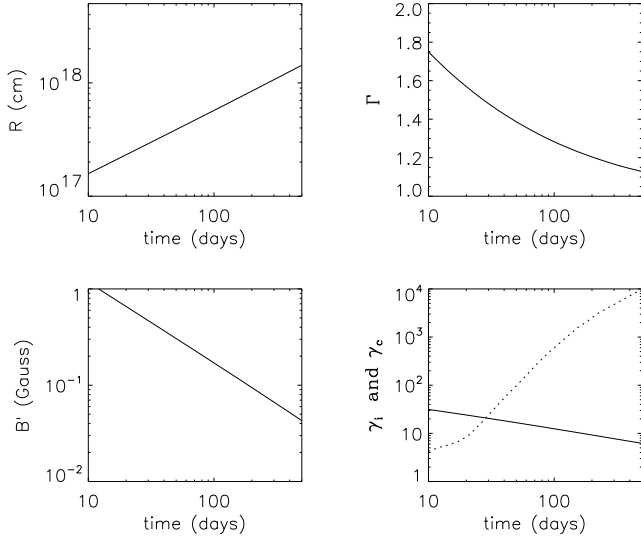


Figure 2. A few of the parameters of the external forward shock are shown in this figure as a function of observer time. Shock front radius (top left), Lorentz factor of the shocked fluid (top right), magnetic field in the comoving frame of shocked fluid (bottom left), and bottom right panel shows γ_i (solid line) & γ_e (dotted line). The energy in the blast wave was taken to be $E = 1.5 \times 10^{53}$ erg (isotropic), the CNM density $n(R) = (400 \text{ cm}^{-3} \times R_{17}^{-2})$, $\epsilon_B = 4.5 \times 10^{-3}$, $\epsilon_e = 0.1$, and $p = 2.3$ for these calculations. The x-ray luminosity was taken to be $L_x = 4 \times 10^{46} \text{ erg/s} (t_{\text{obs}}/20 \text{ days})^{-5/3}$ for $t_{\text{obs}} > 20 \text{ d}$ and constant between 10 and 20 days; x-ray photons passing through the external shock cooled electrons due to IC scatterings and that was the dominant cooling mechanism for electrons radiating at radio/mm frequencies for $\sim 10^2$ days. We note that the uncertainty in γ_e is small as it depends primarily on L_x which is well determined from observations. However, γ_i might be much larger than shown in this figure, particularly for $p \approx 2$ favored by our modeling of the observed data, if the minimum Lorentz factor of electrons accelerated in shocks is larger than the value we have adopted in this paper, viz. $\gamma_i = \epsilon_e(p-2)(\Gamma-1)m_p/[m_e(p-1)]$.

flux which we took for these calculations to decline as $t_{\text{obs}}^{-5/3}$, and the spectrum was taken to be a power law function; $f_\nu \propto \nu^{-0.7}$ for $0.1 \text{ keV} \leq \nu \leq 10 \text{ keV}$ as per Swift/XRT observations⁹ for $t_{\text{obs}} < 40$ days, eg. Saxton et al. (2012). The observed x-ray light curve in reality is much more complicated, and shows rapid fluctuations. However, we do not expect ν_c , and radio light curves, to follow these wild fluctuations because the signal we receive from the external shock at any given fixed observer time is in fact an integral over equal arrival time 3-D hypersurface that has a large radial width so that the effect of x-ray radiation on electron distribution function is averaged over a time duration δt_{obs} of order t_{obs} . The x-ray flux averaged over this time scale is not a smooth power law function, but consists of periods of faster and slower declines. The duration of time when light curve in an observed frequency band is

⁹ Swift/XRT observes photons with energy between 0.3 and 10 keV. However, it would be a remarkable coincidence if the spectrum for Sw J1644+57 starts deviating from the observed power law behavior exactly at the low or the high energy threshold for XRT. The infrared k-band flux at 10 days was 0.03 mJy (Levan et al. 2011) and at the same time the mean 1 keV flux was 0.02 mJy (Zauderer et al. 2013), and that suggests that the XRT spectrum became much harder, perhaps $\nu^{1/3}$, at $\sim 0.1 \text{ keV}$. The flux above 10 keV, however, is rather poorly constrained by observations.

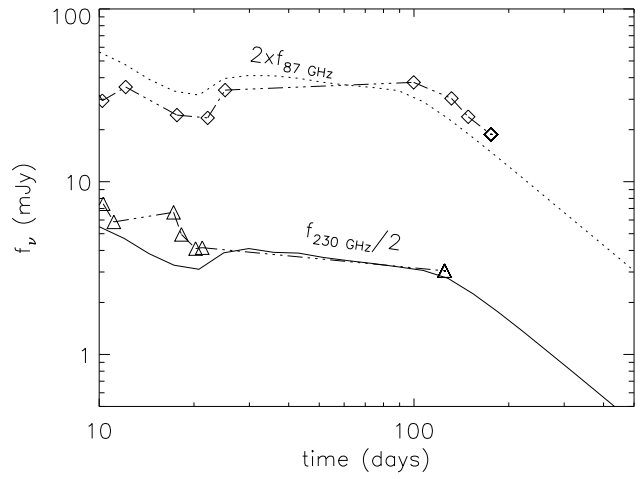


Figure 3. Light curves in frequency bands 230 GHz (solid line) & 87 GHz (dotted curve) calculated for the model described in §3, together with observed data for Sw J1644+57 from Berger et al. (2012) are shown in this figure. The parameters used for these calculations are same as that in Fig. 2 (see fig. 2 caption for details). Light curve before 10 days is not shown here because the wild fluctuation in x-ray flux at earlier times (by more than a factor 10) introduce huge error in our theoretical calculations which is based on a power law decline model for x-ray luminosity for $t_{\text{obs}} > 20$ days, and a constant luminosity for $10 \text{ d} \leq t_{\text{obs}} \leq 20 \text{ d}$. Light curves below 50 GHz are also not shown because of large errors in theoretical calculations at frequencies less than $\sim 2\nu_a$ as discussed in §4.

roughly flat depends on these fluctuations, and for that reason the duration of the flat phase shown in figure 3 should be considered to have an uncertainty of order 20%.

The light curve decline for frequency ν which lies below the synchrotron cooling frequency (ν_c) is easy to obtain using the scalings provided in the §3.2.1. For sub-relativistic shocks, $B' \propto t_{\text{obs}}^{-3/(5-s)}$ (eq. 31), and $\nu_i \propto t_{\text{obs}}^{-(15-4s)/(5-s)}$ (eq. 32), and so the observed flux for $\nu_c > \nu > \max(\nu_a, \nu_i)$ decreases with time as $t_{\text{obs}}^{-[(15-4s)(p-1)-(6-4s)]/2(5-s)}$; for J1644+57, $\nu_c \sim 100 \text{ GHz}$ at $t_{\text{obs}} \sim 10^2 \text{ d}$ (Fig. 4). For $s = 2$ and $p = 2.3$, the light curve decline is expected to be $t_{\text{obs}}^{-1.85}$ which is consistent with the observed decline (see the 87 GHz light curve in Fig. 3 on this page, and also 8.4 — 43 GHz light curves in Fig. 3 of Zauderer et al. 2013).

The reason that we do not show theoretical light curves in fig. 3 for $t_{\text{obs}} < 10$ days is that the x-ray light curve before 10 days is dominated by very large flares — the flux decreased by a factor $\sim 10^2$ between 4 and 6 days — which cannot be captured by a simple power law model used in this paper. A calculation of IC cooling of electrons, and the emergent flux, before 10 days must include these wild fluctuations for the result to be meaningful.

The rise in light curves at lower frequencies (20 GHz or less) and for $10 \text{ d} < t_{\text{obs}} \lesssim 10^2 \text{ d}$ is due to ν_a lying above the band (see Fig. 4). This behavior can be understood using the analytical scalings presented in the last section. However, the error in the calculation of emergent light curves for frequencies $\lesssim 2\nu_a \sim 50 \text{ GHz}$ is very large if the shell of shocked CNM is treated as homogeneous as we have done in this work. The reason is that fluctuations in $L_x(t_{\text{obs}})$ lead to variation of synchrotron absorptivity with angular position and distance from the shock front (due to the effect of X-rays on electron distribution function). And due to the exponential dependence of the emergent flux on the synchrotron optical

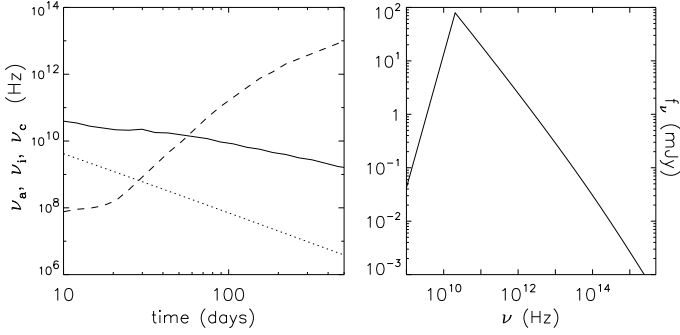


Figure 4. The left panel shows the three synchrotron characteristic frequencies, obtained by numerical calculations, for the same set of parameters as fig. 2; see fig. 2 caption for details; solid line is ν_a , dotted line is ν_i and the dashed curve is ν_c . Note the sharp rise in ν_c , as $\sim t_{obs}^3$, between 20 and 100 days, which is consistent with our analytical estimates (see §3). We note that the uncertainty in the calculation of ν_c is small. However, the actual value of ν_i might be larger than in this figure by 1–2 orders of magnitude for $p \approx 2$ favored by our modeling of the observed data (see caption for Fig. 2 for explanation); good fits to observed light curves (like those shown in fig. 3) can be obtained even when ν_i is much larger than shown in this figure by appropriately rescaling microphysics parameters and changing E and n by a factor ~ 2 . The right side panel shows the spectrum calculated at 52 days. The spectrum above ν_i and ν_c is $\nu^{-0.8}$ even though we took $p = 2.3$. This is due to the fact that when cooling is dominated by IC scatterings of x-ray photons in the K-N regime, the spectrum is $\nu^{-(p-1+\beta)/2}$ instead of $\nu^{-p/2}$; the spectral index for x-ray radiation was $\beta = 0.4$ for $t_{obs} \gtrsim 50$ d (Saxton et al. 2012). The spectrum steepens to $\sim \nu^{-1.15}$ for $\nu \gtrsim 10^{13}$ Hz when the cooling is dominated by synchrotron loss.

depth along the photon trajectory, the error in theoretically calculated light curves is large when these variations are ignored. At sufficiently high frequencies, $\nu \gtrsim 50$ GHz, the optical depth is small and spatial variations of synchrotron absorption are averaged out, and therefore, treating the source as homogeneous is a fine approximation for the calculation of high frequency light curves. This is the reason we show light curves above about 50 GHz in Fig. 3, and not at lower frequencies.

The solutions we are finding have $\min(\nu_i, \nu_c) < \nu_a$, and that might naively suggest that the spectrum below ν_a should be $\nu^{2.5}$ in conflict with the observed spectrum of $\sim \nu^{1.5}$ for $t_{obs} \lesssim 10^2$ d. The fact that the observed spectrum is shallower than ν^2 is already telling us that something is missing. And most likely what that is, is that the jet has some angular structure, and when integration over equal arrival time hyper-surface is carried out to obtain the observed spectrum, it turns out to be softer by $\nu^{0.5}$ — ν^1 than the comoving, instantaneous, spectrum¹⁰.

The infrared flux at 10 days (0.03 mJy, Levan et al. 2011) is roughly of order the theoretically calculated value for parameters

¹⁰ The equal arrival time hyper-surface is a 3-D section of the 4-D space-time with the property that radiation from every point on this hyper-surface arrives at the observer at the same time. The radius (R), γ_i , B' etc. for different points on the hypersurface are in general different for a non-uniform jet, i.e. a jet where energy density, Lorentz factor etc. vary with angle wrt jet axis and distance from the jet surface. It can be shown that an integration over equal arrival time hyper-surface invariably softens the observed spectrum.

used for fitting 230 GHz light curve shown in Fig. 3. The infrared producing electrons have $\gamma'_e \sim 10^4$ and their IC cooling by scattering x-rays photons is highly suppressed due to K-N effect. However, ν_c due to synchrotron cooling is $\sim 10^{13}$ Hz, so the spectrum in this band should be $\sim \nu^{-1}$ if the emission is dominated by the external shock. Levan et al. (2011) report that the infrared light curve declined with time as $\sim t_{obs}^{-3}$ between 5 and 10 days.

This is much too steep to be explained by external shock emission, and we suspect that this fall off suggests that IR radiation is produced by a process internal to the jet. The claim of 7.4 ± 3.5 % linear polarization in the IR K_s -band, at ~ 17 days after the Swift/BAT trigger, by Wiersema et al. (2012) supports this scenario.

A theoretically calculated spectrum for external shock synchrotron radiation at 52 days is shown in Fig. 4. The spectrum above the peak is quite hard, $\sim \nu^{-0.7}$, even though ν_i and ν_c lie below the peak. The reason is that when electrons are cooled by IC scatterings in K-N regime the resulting spectrum is $\nu^{-(p-1+\beta)/2}$ (see §3.1) and not $\nu^{-p/2}$. X-ray data show that β varies with time (Burrows et al. 2011), and that β was about 0.7 for $t_{obs} \lesssim 50$ d and ~ 0.4 for $t \gtrsim 50$ d (Saxton et al. 2012). Therefore, we expect the radio spectrum above the peak to be $\sim \nu^{-0.85}$ at early times, and $\sim \nu^{-0.7}$ at late times, for $p = 2$. The late time radio data are consistent with this expectation, and for $t_{obs} \lesssim 50$ d spectra above the peak are poorly sampled.

4.1 High energy radiation

IC scattering of an x-ray photon of frequency ν_x by an electron of Lorentz factor γ'_i in the external shock produces a high energy photon of energy $\sim 2\gamma'_i \nu_x$. Considering that $\gamma'_i \sim 30$ (Fig. 2), the IC photon energy is ~ 10 MeV, and the expected IC luminosity is $\sim \tau_T L_x \gamma'_i \min(\gamma'_c, \gamma'_i)$; where $\tau_T \sim \sigma_T n(R) R \sim 10^{-5} R_{17} n_{f,2}$ is Thomson optical depth. At $t_{obs} = 10$ d, $L_x \sim 3 \times 10^{46}$ erg s⁻¹, $\gamma'_c \sim 4R_{17}$ & $\gamma'_i \sim 30$ (fig. 2), and therefore we expect IC luminosity to be $\sim 5 \times 10^{43} R_{17}^2 n_{f,2}$ erg s⁻¹. Another way to estimate the luminosity of high energy IC photons follows directly from the fact that IC scatterings of x-ray photons is efficient at cooling electrons at early times, i.e. IC cooling time is less than or of order the dynamical time for $t_{obs} < 20$ d. Hence, the IC luminosity should be roughly equal to the energy luminosity carried by electrons accelerated by the external shock, i.e. $L_{ic} \leq 16\pi\epsilon_e R^2 m_p c^3 n(R) \Gamma^2 \sim 2 \times 10^{44} \epsilon_{e,-1} n_{f,2} R_{17}^2$ erg s⁻¹. There is no data between 1 & 100 MeV for Sw J1644+57 to our knowledge, however, Fermi/LAT provided an upper limit of about 10^{46} erg/s above 100 MeV at 10 d (Burrows et al. 2011). This suggests that n_f , the CNM density at $R = 10^{17}$ cm, cannot be larger than about 10^4 cm⁻³.

4.2 Parameters of the TDE and the external shock

An accurate determination of jet energy and other parameters for Sw J1644+57 should take into consideration the effect of fluctuating L_x on electron distribution, a more detailed treatment of the dynamics than described by equation (20), and the 3D structure of shocked plasma and magnetic fields. But that is beyond the scope of this work¹¹. We show in Fig. 5 an approximate determination

¹¹ The goal of this work is to show that cooling of electrons by x-ray photons passing through the external shock can explain the puzzling, flat, light curves observed in mm/cm bands for $\sim 10^2$ days.

of E (isotropic energy in the external shock), the CNM density, and ϵ_B (energy fraction in magnetic fields) allowed by the multi-wavelength data for Sw J1644+57; see the caption for Fig. 5 for a description of the various observational constraints that were used for the determination of these parameters.

Fermi/LAT upper limit restricts the CNM density at 10^{17} cm to be smaller than $\sim 5 \times 10^3 \text{ cm}^{-3}$ (see §4.1). And according to the radio/mm/infrared data the isotropic energy in the blast wave is $\sim 2 \times 10^{53} \text{ erg}$ which is consistent with estimates obtained using equipartition argument, e.g. Barniol Duran et al. (2013). We note that the uncertainty in these parameters and ϵ_B is a factor of a few. It should be pointed out that the afterglow data we have used for determining energy etc. consists of observations carried out 10 or more days after the TDE. The blast wave Lorentz factor at this time had dropped to $\lesssim 2$, and the angular size of the shocked CNM is perhaps larger by a factor ~ 2 than the jet angle at the smaller radius where x-rays were produced. Thus, the beam corrected energy in the external shock is $\sim 10^{52} \text{ erg}$. A more detailed discussion of beam corrected energy is provided at the end of this sub-section.

We have also looked for the density stratification (s) and find that $s \gtrsim 1.5$ provides a reasonable fit to the available data; $s = 1.5$ density stratification is expected for an advection dominated accretion flow in the neighborhood of a black hole, and $s = 2$ is when outflow determines the CNM density structure.

Although we took $\epsilon_e = 0.1$ for results shown in all of the figures, other values of ϵ_e are allowed by the data as long as we take $E \propto \epsilon_e^{-1}$.

The 1 keV x-ray flux at 610 days after Swift/BAT trigger — for the entire solution space shown in Fig. 5 — is within a factor ~ 2 of the value observed by the Chandra satellite which was 0.7 nJy (Levan & Tanvir, 2012).

Figure 5 shows isotropic equivalent of energy in the blast wave. The true, beam corrected, energy in the explosion can be obtained from this using the blast wave Lorentz factor, Γ_j , and the angular size of the beam. The transformation from an isotropic to a finite opening angle source preserves the specific flux in observer frame which is given here in terms of specific intensity in the source comoving frame ($I'_{\nu'}$)

$$f_{\nu} = \frac{2\pi}{(1+z)^3 \Gamma_j^3} \frac{R^2}{d_A^2} \int_0^{\theta_j} d\theta \frac{\sin \theta \cos \theta I'_{\nu'}}{(1 - v_j \cos \theta)^3}, \quad (50)$$

where θ_j is half-opening angle of the source, z is its redshift, d_A is angular diameter distance, and v_j is the ratio of shock front speed and speed of light. Treating the angular variation of the specific intensity in the jet comoving frame to be small we find

$$f_{\nu} = \frac{\pi I'_{\nu'} R^2}{(1+z)^3 \Gamma_j^3 d_A^2} \left[\frac{2v_j - 1}{v_j^2(1 - v_j)^2} - \frac{2v_j \cos \theta_j - 1}{v_j^2(1 - v_j \cos \theta_j)^2} \right]. \quad (51)$$

The requirement that blast waves of different opening angles produce the same observed flux (f_{ν}) requires appropriate rescaling of $I'_{\nu'}$. Thus, it follows from the above equation that the energy in a blast wave with half opening-angle θ_j , which is proportional to $(1 - \cos \theta_j) \int d\nu' I'_{\nu'}$, is smaller than a spherical blast wave of the same LF by a factor:

$$\frac{E_{\theta_j}}{E_{iso}} = \frac{(1 - \cos \theta_j)}{(1 - v_j)^2} \left[\frac{2v_j - 1}{v_j^2(1 - v_j)^2} - \frac{2v_j \cos \theta_j - 1}{v_j^2(1 - v_j \cos \theta_j)^2} \right]^{-1}. \quad (52)$$

An upper limit to angular size θ_j can be obtained from the maximum transverse speed of spreading in the source comoving frame which is equal to the sound speed of the shock heated plasma given by

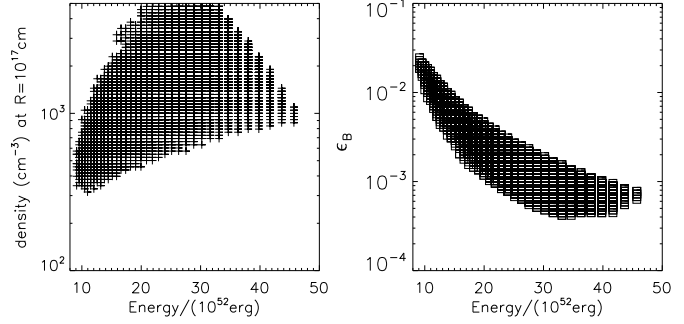


Figure 5. Isotropic blast wave energy (E), CNM density at $R = 10^{17}$ cm, and ϵ_B allowed by the data for Sw J1644+57. The parameters shown in this figure should be considered a rough estimate due to the approximate way we have handled the blast wave dynamics, and used a smooth decline for the x-ray flux passing through the external shock and cooling electrons instead of the highly fluctuating flux Swift/XRT observed. The observational constraints that were used in the determination of parameters are: (1) flux at 230 GHz at 10 days after the tidal disruption was 10 mJy (Berger et al. 2012), (2) $\nu_a = 15$ GHz at 10 days, (3) the flux at the peak of the spectrum at 10^2 days is 50 mJy, (4) an upper limit of $10^{46} \text{ erg s}^{-1}$ for $>10^2 \text{ MeV}$ at 10 days which suggests that $n_f \lesssim 10^4 \text{ cm}^{-3}$ (n_f is density at $R = 10^{17} \text{ cm}$); a tolerance of $\pm 30\%$ was used for all these constraints which reflects the degree of uncertainty of our calculations. We took $L_x = 4 \times 10^{46} \text{ erg/s} (t_{obs}/20 \text{ days})^{-5/3}$ for $t_{obs} > 20 \text{ d}$ and constant between 10 and 20 days, and $\epsilon_e = 0.1$ for these calculations; for $\epsilon_e = 0.5$ these plots look very similar, except that they are shifted to the left by a factor of ~ 5 . The true energy in the blast wave, corrected for its finite angular size, is a factor of ~ 10 smaller than the isotropic energy shown in the figure (see the last part of §4.2 for a detailed discussion).

$$c_s = v_s \left[\frac{2\hat{\gamma}(\hat{\gamma} - 1)}{(\hat{\gamma} + 1)^2} \right]^{1/2}, \quad (53)$$

where $\hat{\gamma}$ is the ratio of specific heats for shocked plasma which is between 4/3 and 5/3 due to the fact that electrons are relativistic whereas protons are sub-relativistic at late times for the external shock of J1644+57, and v_s is the speed of the unshocked fluid wrt the shock front ($v_s > v$; v is the speed of the shocked fluid wrt unshocked CSM). The perpendicular size of the system, $R_{\perp} = R\theta_j$, varies as $dR_{\perp}/dR = c_s/(v_s\Gamma_s)$, if the jet spreads sideways at the speed c_s . Therefore, the angular size of the blast wave when it is at radius R is: $\theta_j < [\theta_0 R_0 + (R - R_0)c_s/(v_s\Gamma_s)]/R \sim (c_s/v_s\Gamma_s)(1 - R_0/R)$; where θ_0 is the angular size when the blast wave was at radius R_0 . Considering that $c_s/v_s \sim 0.5$, that $\Gamma_s \gtrsim 1.3$ (since $v_s > v$), and that R increases by a factor of ~ 10 between 10 and 500 days, the jet angle at ~ 500 days cannot be larger than ~ 0.3 radian; most likely $\theta_j \sim 0.2$ at 500 days since the sideways expansion speed becomes c_s only when the shocked plasma cools down to a temperature substantially lower than the temperature it had just behind the shock-front¹².

¹² Kumar & Granot (2003) using 1-D hydro simulations found little evidence for sideways spreading for a beamed jet interacting with ISM during the relativistic phase, and the 2-D simulation of Zhang & MacFadyen (2009) found the jet angle at 500d — when the blast wave was sub-relativistic — to be close to 0.2 radian which should be independent of the choice of the initial jet angle.

For $\Gamma_j = 1.2$ and $\theta_j = 0.2$, E_{θ_j} is smaller than an equivalent spherical blast wave by a factor 4.3, and for $\Gamma_j = 1.5$, and $\theta_j = 0.2$, E_{θ_j} is smaller by a factor ~ 7 . The isotropic energy we show in Fig. 5 is for $\epsilon_e = 0.1$. The energy in the external shock is smaller by a factor $\sim 10\epsilon_e$ for a larger ϵ_e . So the isotropic energy shown in Fig. 5 should be divided by a factor ~ 10 (if $\epsilon_e = 0.2$, which is very likely) in order to obtain the true energy in J1644+57 as required by the radio/mm data. Therefore, the total energy in the blast wave of J1644+57 is estimated to be of order 10^{52} erg which is consistent with the amount obtained independently from the x-ray data.

4.3 A puzzling drop in ν_a between 5 & 10 days

According to Berger et al. (2012) the synchrotron-absorption frequency (ν_a) dropped by a factor 10 between 5 and 10 days after the tidal disruption event Sw J1655+57. If these observations are correct¹³ then this result essentially rules out any shock model, with or without continuous energy injection, for radio emission unless some mechanism external to the shock led to a drastic change to the electron energy and magnetic fields in shocked plasma between 5 and 10 days. To understand this result we make use of equation (46) for ν'_a :

$$\nu'_a \gamma'_e(\nu'_a) \propto B' N_e(\geq \gamma'_e) \text{ or } \nu_a \propto \Gamma [B'^{3/2} N_e(\geq \gamma'_e)]^{0.4} \quad (54)$$

where $\gamma'_e(\nu'_a)$ is the Lorentz factor of electrons that have characteristic synchrotron frequency ν'_a , and $N_e(\geq \gamma'_e)$ is the column density of electrons that radiate above ν'_a . The right hand side of the first equation is proportional to the synchrotron flux at ν'_a in the comoving frame of the source when synchrotron absorption is ignored, and in the second equation we have considered the case where $\nu'_a > \min(\nu'_i, \nu'_c)$ (other cases are straightforward to consider). For any external shock model, with or without energy injection and arbitrary CNM density stratification, Γ , B' and N_e are smooth functions of time (see §3). Since $\Gamma \propto t_{obs}^{-(3-s)/(8-2s)}$ (eq. 26), the most change we can expect for Γ between 5 and 10 days is a factor $2^{3/8} \sim 1.3$ for a $s = 0$ medium; similarly, $B' \propto \Gamma R^{-s/2}$ cannot change much during this time in the absence of an external agency at work. And N_e , which depends on the number of electrons in the CNM swept up by the shock, is typically an increasing function of time and hence its effect on ν'_a is to increase it¹⁴. We know empirically that $N_e(\geq \gamma'_e) B' \propto f(\nu_a)/\Gamma$ decreased by a factor ~ 3 between 5 and 10 days for Sw J1644+57 (see fig. 2 of Berger et al. 2012), and that by itself can only account for a decrease of ν_a by a factor $\lesssim 2$. We see, therefore, that unless there is a dramatic change in B' and/or $\gamma'_e(\nu'_a)$ on a short time scale of $\delta t_{obs}/t_{obs} = 1$ — which is not possible in external shocks without a powerful radiation front passing through it or some such mechanism — ν_a cannot drop by a factor ~ 10 between 5 and 10 days that is observed for Sw J1644+57; any addition of energy to a decelerating shock only makes the problem worse.

¹³ We would not be surprised if it were to turn out that the drop in ν_a has been overestimated by observers by a factor 2–3. The spectrum reported by Berger et al. (2012) at $t_{obs} = 10$ d has no frequency coverage between 15 and 80 GHz. It is possible that the actual peak was at ~ 50 GHz, in which case ν_a at 10 d has been underestimated by a factor ~ 3 .

¹⁴ If a shock were to run into a dense cloud, that would cause ν_a to increase. And when a shock suddenly encounters a zero density medium, the shocked plasma undergoes adiabatic expansion and then γ'_e , B' , and $N'_e(\geq \nu'_a)$ decrease with time. It is easy to show that the net effect of adiabatic expansion is a slight decrease of ν_a in time interval $t_{obs} - 2t_{obs}$.

It is probably no coincidence that the x-ray luminosity of Sw J1644+57 fell by a factor ~ 50 during the same time period that ν_a dropped by a factor 10. When a highly luminous x-ray front was passing through the external shock ($t_{obs} \lesssim 6$ d), electrons in the region were cooled by IC scatterings of x-rays to a Lorentz factor of order unity in less than one dynamical time (see eq. 9). The sharp drop in x-ray luminosity during 6 to 8 days by a factor 50 reduced the IC cooling of electrons and raised γ'_e by the same factor. As we can see from equation (54) a rising electron temperature helps to lower ν_a , however, the effect on $\gamma'_e(\nu'_a)$ is much smaller. Ultimately, a sharp drop in B' is needed to account for the observed decrease of ν_a as can be seen from the second part of equation (54). We suspect that a sharp drop in L_x leads to a smaller B' . One possible way this might occur is that while L_x is large, or jet power is high, the interface separating the shocked jet and the shocked CNM is Rayleigh-Taylor unstable and the turbulence associated with this instability produces strong magnetic fields. Currents driven in the shocked CNM by high L_x might be another way to generate close to equipartition magnetic field in the region where radio/mm emission is produced. However, a connection between L_x and magnetic field generation is just a speculation at this point¹⁵.

5 CONCLUDING REMARKS

An interesting puzzle is posed by the radio/mm data for the tidal disruption event Swift J1644+57: light curves in frequency bands that lie above the synchrotron characteristic peak frequencies, i.e. $\nu > 10$ GHz, are roughly flat for 10^2 days rather than decline with time as $\sim t_{obs}^{-1}$ as one would expect for radiation produced in the external shock. Berger et al. (2012) suggested that the flat light curves are due to continued addition of energy to the external shock for 10^2 days. This requires about 10 times more energy to be added at late times than is seen in x-rays, and that is worrisome. We have described in this paper a simple model for flat light curves that does not require adding any extra energy to the decelerating shock wave. The flat light curves, instead, are a result of efficient cooling of electrons in the external shock by IC scatterings of x-ray photons that pass through the external shock region on their way to us (Fig. 1). The IC cooling becomes weaker with time as the x-ray flux declines and that is the origin of radio/mm light curve flatness. This model can account for the radio and milli-meter data (temporal decay as well as spectra), and is consistent with $> 10^2$ MeV upper limit provided by Fermi/LAT.

The angular size of the x-ray beam should not be much smaller than the size of the external shock region during the initial $\sim 10^2$ days for the IC cooling model to work; otherwise only a fraction of shock accelerated electrons will be exposed to IC cooling, and the effect described here is weakened. The angular spreading of blast wave is discussed in §4.2 where it is shown that even at $t = 500$ d the angular size of the jet is no more than a factor 2 larger than its size at 10 d. Moreover, the decline of the late time radio/mm light curves as $\sim t_{obs}^{-1.8}$ for $t_{obs} \gtrsim 200$ days (Zauderer et al. 2013; Fig. 3) requires — in the framework of synchrotron radiation from a decelerating blast wave model — the angular spreading to be very weak; the light curve decline for a sub-relativistic blast wave of a constant opening angle, for $p = 2.3$ & $s = 2$, can be easily

¹⁵ We do not expect the magnetic field to continue to decline with L_x indefinitely. The reason for this is that below a certain threshold x-ray luminosity magnetic field generation in external forward shock proceeds by Weibel mechanism, or some other instability, that is not affected by L_x .

shown to be $t_{obs}^{-1.85}$ using formulae provided in §3.2. In fact, considering the *naturalness* of this model — it is unavoidable that x-ray photons pass through the external shock and cool electrons — and its clear cut, robust, implications for external shock light curves, it is not unreasonable to conclude from the data for this TDE that sideways spreading speed is at best modest for sub-relativistic blast waves as long as $\Gamma \gtrsim 1.1$.

The model predicts a connection between the observed x-ray light curve and the temporal and spectral properties of radio and mm radiation from Sw J1644+57. It requires more extensive numerical modeling than presented in this paper to explore this connection in detail, which can then be confronted with the extensive data for this remarkable event.

Barniol Duran & Piran (2013) have suggested two broad class of models for Sw J1644+57 using equipartition arguments within the context of synchrotron emission, but without considering the IC cooling of electrons. The first scenario consists of one jet that is responsible for both the X-ray and the radio emission. The second scenario invokes two sources: a narrow relativistic jet to produce X-rays, and a quasi-spherical, mildly relativistic, source to produce the radio emission. Both models require the energy available to electrons for synchrotron radiation to increase with time, but Barniol Duran & Piran (2013) argue that the total energy in the radio source could be constant. The model suggested in the present work roughly corresponds to the first scenario, with a constant total energy, where the energy fraction available to electrons for synchrotron radiation increases with time as the x-ray luminosity decreases and the IC losses weaken.

ACKNOWLEDGEMENTS

We thank Patrick Crumley and Roberto Hernandez for comments on the manuscript.

REFERENCES

- Ayal S., Livio M., Piran T., 2000, ApJ, 545, 772
 Barniol Duran, R., Nakar, E., Piran, T., 2013, ApJ, 772, 78
 Barniol Duran, R. & Piran, T., 2013, ApJ, 770, 146
 Berger, E. et al. 2012, ApJ, 748, 36
 Bloom, J.S. et al. 2011, Science, 333, 203
 Bower, G.C. 2011, ApJ, 732, L12
 Burrows, D.N. et al. 2011, Nature, 476, 421
 Cenko, S.B. et al. 2011, ApJ, 753, 77
 Chevalier R.A. & Li Z.-Y. 2000, ApJ, 536, 195
 De Colle, F., Guillochon, J., Naiman, J., Ramirez-Ruiz, E., 2012, ApJ, 760, 103
 Evans C.R. & Kochanek C.S., 1989, ApJ, 346, L13
 Gezari, S. et al. 2012, Nature, 485, 217
 Giannios, D. & Metzger, B.D. 2011, MNRAS, 416, 2102
 Goodman J., Lee H. M., 1989, ApJ, 337, 8
 Granot, J. & Sari, R. 2002, ApJ, 568, 820
 Kumar, P. 2000, ApJ, 538, L125
 Kumar, P., Granot, J. 2003, ApJ, 591, 1075
 Lacy, J. H., Townes, C. H., Hollenbach, D. J. 1982, ApJ, 262, 120
 Levan, A.J. et al. 2011, Science, 333, 199
 Levan, A. J., Tanvir, N. 2012, The Astronomers Telegram, 4610, 1
 Liu, D., Pe'er, A., Loeb, A., 2012, ApJ, submitted (arXiv:1211.5120)
 Meszaros P. & Rees M.J. 1994, MNRAS, 269, 41
 Metzger, B.D., Giannios, D. & Mimica, P. 2012, MNRAS, 420, 3528
 Magorrian J., Tremaine S., 1999, MNRAS, 309, 447
 Nakar, E., Ando, S., Sari, R. 2009, ApJ, 703, 675
 Panaitescu A., Kumar P. 2000, ApJ, 543, 66

- Rees, M.J. 1988, Nature, 333, 523
 Rybicki, G.B., Lightman, A. P. 1986, Radiative Processes in Astrophysics
 Saxton, C.J. et al. 2012, MNRAS, 422, 1625
 Strubbe, L.E., Quataert, E. 2009, MNRAS, 400, 2070
 Strubbe L. E., Quataert E., 2011, MNRAS, 415, 168
 Tchekhovskoy, A., Metzger, B.D., Giannios, D., Kelley, L.Z., 2013, MNRAS, submitted (arXiv:1301.1982)
 Wang, J. & Merritt, D. 2004, ApJ, 600, 149
 Wiersema, K. et al. 2012, MNRAS, 421, 1942
 Zauderer, B.A. et al. 2011, Nature, 476, 425
 Zauderer, B.A. et al. 2013, ApJ, 767, 152
 Zhang, W., MacFadyen, A.I. 2009, ApJ, 698, 1261